

Analytic solutions of multiple moving cracks in an orthotropic layer bonded to an orthotropic FGM coating



Mojtaba Ayatollahi^{a,*}, Rasul Bagheri^b, Mahsa Nourazar^a,
Mojtaba Mahmoudi Monfared^c, S. Mahmoud Mousavi^d

^a Faculty of Engineering, University of Zanjan, P.O. Box 45195-313, Zanjan, Iran

^b Department of Mechanical Engineering, Karaj Branch, Islamic Azad University, Alborz, Iran

^c Department of Mechanical Engineering, Hashtgerd Branch, Islamic Azad University, P.O. Box 33615-178, Alborz, Iran

^d Department of Civil and Structural Engineering, Aalto University, P.O. Box 12100, FI - 00076, Finland

ARTICLE INFO

Keywords:

Antiplane
Orthotropic strip
Imperfect FGM orthotropic coating
Multiple cracks
Stress intensity factors

ABSTRACT

In this paper, the dynamic behavior of an orthotropic substrate weakened by moving cracks and reinforced by a non-homogenous coating is studied. First, the solution to the screw dislocation in an orthotropic strip with imperfect orthotropic functionally graded coating is obtained. Then, for the anti-plane analysis of cracks, the screw dislocations are distributed along the crack lines and the dislocation solution is used to derive integral equations for dislocation density functions on the surface of cracks. The effects of non-homogeneity parameters, geometrical parameters and bonding coefficient on the stress intensity factors are investigated.

© 2016 Elsevier Inc. All rights reserved.

1. Introduction

One of the important potential applications of functionally graded materials (FGMs) is in the area of thermal barrier coatings (TBCs) technology. Used as coating and interfacial zones, FGMs help to reduce mechanically and thermally induced stresses caused by the material property mismatch and to improve the bonding strength. Typical applications of FGMs include thermal barrier coatings of high temperature components in gas turbines, surface hardening for tribological protection, and as inter-layers in microelectronic and optoelectronic components. While the ceramic in an FGM supports thermal barrier effects and protects the metal from oxidation and corrosion, the metal increases the strength of the FGM. The study of FGMs reveals that the residual stress can be effectively relaxed by using an FGM coating in a coating–substrate composite.

In many engineering applications, non-homogeneous structures may be subjected to dynamic loadings. The dynamic manipulation of such structures may lead to crack formation and eventually the failures of the structures. During the last decade, the problem of dynamic crack propagation in a coating–substrate structures has been studied by many other researchers, both theoretically and experimentally. The knowledge of crack propagation in non-homogeneous orthotropic materials is important in designing components made of FGMs and improving their fracture toughness. The problems of crack propagation at constant speed can be classified into three categories depending on the boundary conditions [1]. The prototype problem of the first category is the two-dimensional Yoffe problem of a crack with fixed length propagating in a body.

* Corresponding author. Tel: +98-241-515-2488; Fax: +98-241-228-3204.

E-mail addresses: mo.ayatollahy@gmail.com, mo_ayatollahy@yahoo.com (M. Ayatollahi).

The effect of crack propagation velocity on the stress intensity factor has been studied by Sih [2]. The solution for this complex elastodynamic problem has been sought under various assumptions. Later, Sih and Chen [3] studied the dynamic behavior of a moving crack in layered composites while Danyluk and Singh [4] obtained closed form solutions for a finite length crack moving with constant velocity in an orthotropic layer. Wang and Meguid [5] introduced a theoretical and numerical treatment of a finite crack propagating in an interfacial layer with spatially varying elastic properties under the anti-plane loading. Wang and Williams [6] analyzed the dynamic crack propagation in tapered double cantilever beam specimens with the use of beam theory and the finite element method.

The dynamic crack propagation in FGMs under the plane elastic deformation using Fourier transform technique was investigated by Meguid et al. [7]. Jiang and Wang [8] studied the dynamic behavior of a Yoffe type crack propagating in a functionally graded interlayer bonded to dissimilar half planes. Chi and Chung [9] obtained the stress intensity factor for cracked multi-layered and functionally graded material coatings of a coating–substrate composite. The dynamic stress intensity factor and strain energy density for moving crack in an infinite strip of functionally graded material subjected to anti-plane shear was determined by Bi et al. [10]. A finite crack with constant length propagating in the functionally graded orthotropic strip under in plane loading was investigated by Ma et al. [11]. Therein, the effects of material properties, thickness of the functionally graded orthotropic strip and the speed of the crack propagating upon the dynamic fracture behavior were studied.

Das [12] investigated the interaction between three moving collinear Griffith cracks under anti-plane shear stress situated at the interface of an elastic layer overlying a different half plane. The problem of a Griffith crack of constant length propagating at a uniform speed in a non-homogeneous plane under uniform load was studied by Singh et al. [13]. Wang and Han [14], considered the problem of a moving crack in a non-homogeneous material strip. They found that the maximum anti-plane shear stress around the crack tip is a suitable failure criterion for moving cracks. In another paper, Wang and Han investigated the dynamic behavior of a crack moving at the interface between an FGM layer and homogeneous substrate [15]. The finite crack with constant length (Yoffe-type crack) propagating in a functionally graded strip with spatially varying elastic properties between two dissimilar homogeneous layers under in-plane loading was studied by Cheng and Zhong [16]. The dynamic delamination problems have been studied for steady-state crack growth in fiber reinforced composites by Gereco and Lonetti [17]. Bruno et al. [18] also investigated the dynamic crack problem in composite laminates. They used beam and interface methodologies to obtain crack behavior in the steady-state condition. Cheng et al. [19] investigated the problem of a finite crack with constant length propagating in a functionally graded coating bonded to a homogeneous substrate under anti-plane loading.

In the most of these studies, the interfaces between the coating and the substrate are often assumed to be perfect; however, the assumption of perfect bonding is sometimes inadequate. Bagheri et al. [20] solved the anti-plane shear problem of orthotropic strips with multiple stationary cracks and imperfect FGM coating. They studied the effects of material properties of the FGM layer and the spring constant of imperfect boundary on the stress fields. They have employed the distributed dislocation technique for this purpose. This technique is capable of the analysis of multiple defects. This static analysis is aimed to be extended to the moving crack in this paper.

The main objective of this study is to apply the distributed dislocation technique for the stress analysis of multiple moving cracks with arbitrary arrangement in a graded orthotropic layer imperfectly bonded to an orthotropic substrate. The elastic stiffness constants and mass density of materials are assumed to vary exponentially perpendicular to the direction of the crack propagation. The Galilean transformation is employed to express the wave equations in terms of coordinates that are attached to the moving crack. Numerical calculations are carried out for the effects of the crack speed, non-homogeneity parameters and bonding coefficient on the stress intensity factors.

2. Dislocation solution

Consider an orthotropic homogeneous substrate of thickness h_2 bonded to a functionally graded orthotropic coating of thickness h_1 (Fig. 1). In multiple cracks problems, the distributed dislocation technique is often used for treating cracks with smooth geometries [21]. This method relies on the knowledge of stress field due to a single dislocation in the region of interest. However, determining stress fields due to a single dislocation in the region has been a major obstacle to the utilization of this method. We now take up this task for an orthotropic strip with imperfect functionally graded orthotropic coating containing a moving screw dislocation. For the anti-plane analysis, there is only out-of-plane displacement W in each elastic layer, and other two elastic displacements u and v oriented in the x - and y -axes vanish. Precisely, in the homogeneous elastic layers, the basic equations which govern the anti-plane deformation of the layers can be expressed in a fixed Cartesian coordinate system (X, Y) as

$$\begin{aligned} G_X(Y) \frac{\partial^2 W}{\partial X^2} + G_Y(Y) 2\lambda \frac{\partial W}{\partial Y} + G_Y(Y) \frac{\partial^2 W}{\partial Y^2} &= \rho_1(Y) \frac{\partial^2 W}{\partial t^2} \quad 0 < Y < h_1, \\ \mu_X \frac{\partial^2 W}{\partial X^2} + \mu_Y \frac{\partial^2 W}{\partial Y^2} &= \rho_0 \frac{\partial^2 W}{\partial t^2} \quad -h_2 < Y < 0. \end{aligned} \quad (1)$$

where $G_X(Y)$ and $G_Y(Y)$ are material constants of FGM orthotropic layer, and parameters μ_X and μ_Y are the shear moduli of elasticity of the orthotropic strip in the x - and y -directions, respectively. It should be noted that body forces are neglected in the present work. For simplicity, we will assume that the shear moduli $G_X(Y)$, $G_Y(Y)$ and mass density $\rho_1(Y)$ of functionally

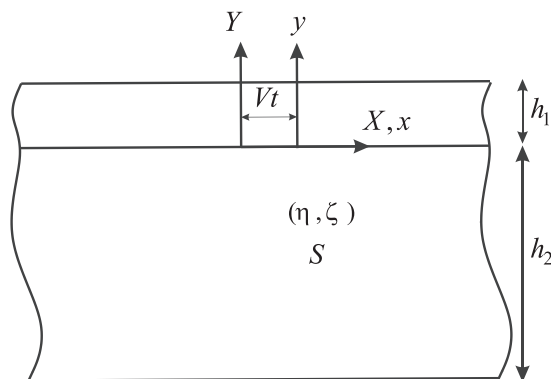


Fig. 1. Schematic view of layers weakened by screw dislocation.

graded orthotropic layer read

$$\begin{aligned} G_i(Y) &= G_i e^{2\lambda Y} \quad i = x, y. \\ \rho_1(Y) &= \rho_1 e^{2\lambda Y} \end{aligned} \quad (2)$$

where G_i and ρ_1 are material constants at $Y = 0$. In order to overcome the complexity of the mathematics involved, Eq. (2) introduces a special class of non-homogeneous materials in which the property variations are in the same proportion and have exponential forms. This simplifying assumption results in analytical solution for equilibrium equations. Further, we assume

$$C_T = \sqrt{\mu_X/\rho_0}, \quad C_p = \sqrt{G_Y/\rho_1}, \quad f = \sqrt{\mu_X/\mu_Y}, \quad g = \sqrt{G_X/G_Y} \quad (3)$$

For the current problem, it is convenient to introduce the following Galilean transformation

$$X = x + Vt, \quad Y = y, \quad \frac{\partial}{\partial t} = V \frac{\partial}{\partial x}. \quad (4)$$

with x and y being a translating coordinate system, which is attached to the propagating dislocation. It is, however, assumed that the propagation of the crack has prevailed for such a long time that the stress distribution around its tip is time invariant in the translating reference frame. Then Eq. (1) can be written within the new coordinate system (x, y) as

$$\begin{aligned} \gamma_1^2 \frac{\partial^2 w}{\partial x^2} + \frac{\partial^2 w}{\partial y^2} + 2\lambda \frac{\partial w}{\partial y} &= 0 \quad 0 < y < h_1 \\ \gamma_2^2 \frac{\partial^2 w}{\partial x^2} + \frac{\partial^2 w}{\partial y^2} &= 0 \quad -h_2 < y < 0 \end{aligned} \quad (5)$$

while $\gamma_1^2 = (g^2 - V^2/C_p^2)$ and $\gamma_2^2 = f^2(1 - V^2/C_T^2)$. Eq. (5) governs the steady state solution. For the dislocation problem, since no traction is applied on both the upper boundary $y = h_1$ and the lower boundary $y = -h_2$, the following conditions must be satisfied

$$\sigma_{zy}(x, h_1) = 0, \quad \sigma_{zy}(x, -h_2) = 0 \quad (6)$$

The stress and displacement fields for the screw dislocation in Fig. 1 should also satisfy the following conditions

$$\begin{aligned} w(x, \zeta^+) - w(x, \zeta^-) &= b_z H(x - \eta) \\ \sigma_{zy}(x, \zeta^+) &= \sigma_{zy}(x, \zeta^-) \\ \sigma_{zy}(x, 0^+) &= \sigma_{zy}(x, 0^-) = k[w(x, 0^+) - w(x, 0^-)] \end{aligned} \quad (7)$$

Here, $H(x)$ is the Heaviside step-function and b_z is the magnitude of the Burgers vector for the screw dislocation. Moreover, the imperfect bonding conditions is modeled as an interfacial spring with k being the spring stiffness at the interface. For $k = 0$, the problem reduces to an orthotropic strip without reinforcement and $k = \infty$ indicates that the coating and the substrate are perfectly bonded.

The solutions to Eq. (5) subjected to the above-mentioned conditions (6) and (7) are achieved by means of the Fourier transform. The details are not given here. Substituting the obtained displacement fields obtained into the constitutive equations, the stress field in the coating reads

$$\begin{aligned} \sigma_{zx} &= \frac{G_x k \mu_y b_z e^{\lambda y}}{\pi} \int_0^\infty [\beta \cos h(\beta(y - h_1)) + \lambda \sin h(\beta(y - h_1))] \frac{\alpha \sin h[\alpha(\zeta + h_2)]}{sE(s)} \cos(s(x - \eta)) ds \quad 0 < y < h_1 \\ \sigma_{zy} &= \frac{G_y k \mu_y b_z e^{\lambda y}}{\pi} \int_0^\infty (\beta^2 - \lambda^2) \sin h(\beta(y - h_1)) \frac{\alpha \sin h[\alpha(\zeta + h_2)]}{s^2 E(s)} \sin(s(x - \eta)) ds \quad 0 < y < h_1 \end{aligned} \quad (8a)$$

Following a routine methodology, the stress field in the substrate is given by:

$$\begin{aligned}
 \sigma_{zx} &= -\frac{\mu_x b_z}{\pi} \int_0^{+\infty} [kG_y(\beta^2 - \lambda^2) \sin h(\beta h_1) \sin h(\alpha y) - \mu_y \alpha \cos h(\alpha y) \{k\beta \cos h(\beta h_1) - k\lambda \sin h(\beta h_1) \\
 &\quad + G_y(\beta^2 - \lambda^2) \sin h(\beta h_1)\}] \frac{\sin h[\alpha(\zeta + h_2)]}{sE(s)} \cos(s(x - \eta)) ds \quad \zeta < y < 0 \\
 \sigma_{zy} &= -\frac{\mu_y b_z}{\pi} \int_0^{+\infty} [kG_y(\beta^2 - \lambda^2) \sin h(\beta h_1) \alpha \cos h(\alpha y) - \mu_y \alpha^2 \sin h(\alpha y) \{k\beta \cos h(\beta h_1) - k\lambda \sin h(\beta h_1) \\
 &\quad + G_y(\beta^2 - \lambda^2) \sin h(\beta h_1)\}] \frac{\sin h[\alpha(\zeta + h_2)]}{s^2 E(s)} \sin(s(x - \eta)) ds \quad \zeta < y < 0 \\
 \sigma_{zx} &= -\frac{\mu_x b_z}{\pi} \int_0^{+\infty} [kG_y(\beta^2 - \lambda^2) \sin h(\beta h_1) \cos h(\alpha \zeta) - \mu_y \alpha \sin h(\alpha \zeta) \{k\beta \cos h(\beta h_1) - k\lambda \sin h(\beta h_1) \\
 &\quad + G_y(\beta^2 - \lambda^2) \sin h(\beta h_1)\}] \frac{\cos h[\alpha(y + h_2)]}{E(s)s} \cos(s(x - \eta)) ds \quad -h_2 < y < \zeta \\
 \sigma_{zy} &= -\frac{\mu_y b_z}{\pi} \int_0^{+\infty} [kG_y(\beta^2 - \lambda^2) \sin h(\beta h_1) \cos h(\alpha \zeta) - \mu_y \alpha \sin h(\alpha \zeta) \{k\beta \cos h(\beta h_1) - k\lambda \sin h(\beta h_1) \\
 &\quad + G_y(\beta^2 - \lambda^2) \sin h(\beta h_1)\}] \frac{\alpha \sin h[\alpha(y + h_2)]}{E(s)s^2} \sin(s(x - \eta)) ds \quad -h_2 < y < \zeta
 \end{aligned} \tag{8b}$$

where parameters β and α read

$$\beta = \sqrt{\lambda^2 + s^2 \gamma_1^2}, \alpha = \gamma_2 s \tag{9a}$$

In the region $0 \leq y \leq h_1$, the integrands of Eq. (8a) decay sufficiently rapid as $s \rightarrow \infty$. Therefore, the integrals can be evaluated numerically. In order to determine the possible singular behavior of (8b) in the region $-h_2 \leq y \leq 0$, the behavior of the kernels should to be examined. For this, it is sufficient to determine and separate those leading terms in the asymptotic expansion of kernels as $s \rightarrow \infty$ that would lead to unbounded integrals. As expected, the stress fields are singular at the location of dislocation. The stress components in Eq. (8b) can be recast as follows:

$$\begin{aligned}
 \sigma_{zx} &= -\frac{\mu_x b_z}{2\pi} \left\{ \frac{\gamma_2(\zeta - y)}{r^2} + \int_0^{+\infty} \left([2kG_y(\beta^2 - \lambda^2) \sin h(\beta h_1) \sin h(\alpha y) + 2\mu_y \alpha \cos h(\alpha y) \right. \right. \\
 &\quad \times \{k\lambda \sin h(\beta h_1) - k\beta \cos h(\beta h_1) - G_y(\beta^2 - \lambda^2) \sin h(\beta h_1)\}] \frac{\sin h[\alpha(\zeta + h_2)]}{E(s)s} \\
 &\quad \left. \left. + e^{-s\gamma_2(y-\zeta)} \right) \cos(s(x - \eta)) ds \quad \zeta < y < 0 \right. \\
 \sigma_{zy} &= -\frac{\mu_y b_z}{\pi} \left\{ \frac{\gamma_2(x - \eta)}{r^2} + \int_0^{+\infty} \left([kG_y(\beta^2 - \lambda^2) \sin h(\beta h_1) \alpha \cos h(\alpha y) + \mu_y \alpha^2 \sin h(\alpha y) \right. \right. \\
 &\quad \times \{k\lambda \sin h(\beta h_1) - k\beta \cos h(\beta h_1) - G_y(\beta^2 - \lambda^2) \sin h(\beta h_1)\}] \frac{\sin h[\alpha(\zeta + h_2)]}{E(s)s^2} \\
 &\quad \left. \left. - \gamma_2 e^{-\gamma_2 s(y-\zeta)} \right) \sin(s(x - \eta)) ds \right\} \zeta < y < 0 \\
 \sigma_{zx} &= -\frac{\mu_x b_z}{2\pi} \left\{ \frac{\gamma_2(\zeta - y)}{r^2} + \int_0^{+\infty} \left([2kG_y(\beta^2 - \lambda^2) \sin h(\beta h_1) \cos h(\alpha \zeta) + 2\mu_y \alpha \sin h(\alpha \zeta) \right. \right. \\
 &\quad \times \{k\lambda \sin h(\beta h_1) - k\beta \cos h(\beta h_1) - G_y(\beta^2 - \lambda^2) \sin h(\beta h_1)\}] \frac{\cos h[\alpha(y + h_2)]}{E(s)s} \\
 &\quad \left. \left. - e^{-s\gamma_2(\zeta-y)} \right) \cos(s(x - \eta)) ds \right\} -h_2 < y < \zeta \\
 \sigma_{zy} &= -\frac{\mu_y b_z}{2\pi} \left\{ \frac{\gamma_2(x - \eta)}{r^2} + \int_0^{+\infty} ([2kG_y(\beta^2 - \lambda^2) \sin h(\beta h_1) \alpha \cos h(\alpha \zeta) + 2\mu_y \alpha^2 \sin h(\alpha \zeta) \right. \\
 &\quad \times \{k\lambda \sin h(\beta h_1) - k\beta \cos h(\beta h_1) - G_y(\beta^2 - \lambda^2) \sin h(\beta h_1)\}] \frac{\sin h[\alpha(y + h_2)]}{E(s)s^2} \\
 &\quad \left. \left. - \gamma_2 e^{-\gamma_2 s(\zeta-y)} \right) \sin(s(x - \eta)) ds \right\} -h_2 < y < \zeta
 \end{aligned} \tag{9b}$$

where $r = \sqrt{(x - \eta)^2 + \gamma_2^2(y - \zeta)^2}$. All integrals in Eq. (9a) decay reasonably fast as $s \rightarrow \infty$. Consequently, the integrals are regular and stress fields exhibit the familiar Cauchy type singularity at the dislocation core. It is straightforward to verify Eq. (9b), in the particular case of static screw dislocation. Letting $V = 0$ in Eq. (9b), the above solutions are identical to those given in [22].

3. Moving crack formulation

The distributed dislocation technique has been used by several investigators for the analysis of cracked bodies; see e.g. Weertman [23]. Employing this technique, we employ the solution of the screw dislocation accomplished in the preceding section to analyze layers weakened by several cracks and subjected to anti-plane load.

The moving cracks configurations with respect to coordinates x and y may be described in parametric form as

$$\begin{aligned} x_i &= x_{0i} + l_i s \\ y_i &= y_{0i} \quad i = 1, 2, \dots, N \quad -1 \leq s \leq 1 \end{aligned} \quad (10)$$

while l_i is the half-length of the i th crack. We consider local coordinate systems moving on the face of i th crack. The traction on the surface of the i th crack is

$$\sigma_{nz}(x_i, y_i) = \tau_0 \quad (11)$$

Suppose dislocations with unknown dislocation density $B_{zj}(p)$ are distributed on the infinitesimal segment dl_j on the surface of the i th crack. The traction component on the face of i th crack due to the presence of the above-mentioned distribution of dislocations on all N cracks surface yield

$$\sigma_{nz}(x_i(s), y_i(s)) = \sum_{j=1}^N \int_{-1}^1 k_{ij}(s, p) l_j B_{zj}(p) dp \quad i = 1, 2, \dots, N. \quad (12)$$

The system of integral Eq. (12) is Cauchy singular for $s \rightarrow p$. By virtue of Buckner's superposition theorem the left hand-side of Eq. (12) is identical to the traction with opposite sign obtained from (11). In order to determine the singular behavior of Eq. (12), the behavior of kernel should to be examined. Considering (Eq. (9), the kernels of integral Eq. (12) read

$$\begin{aligned} K_{ij}(s, p) &= -\frac{\mu_y}{\pi} \left\{ \frac{\gamma_2(x_i(s) - x_j(p))}{r_{ij}^2(s, p)} + \int_0^{+\infty} \left([kG_y(\beta^2 - \lambda^2) \sin h(\beta h_1) \alpha \cos h(\alpha y_i(s)) \right. \right. \\ &\quad \left. \left. + \mu_y \alpha^2 \sin h(\alpha y_i(s)) \{k\lambda \sin h(\beta h_1) - k\beta \cos h(\beta h_1) - G_y(\beta^2 - \lambda^2) \sin h(\beta h_1)\} \right] \right. \\ &\quad \left. \times \frac{\sin h[\alpha(y_j(p) + h_2)]}{E(s)s^2} - \gamma_2 e^{-\gamma_2 s(y_i(s) - y_j(p))} \right\} \sin(s(x_i(s) - x_j(p))) ds \quad \zeta < y < 0 \\ K_{ij}(s, p) &= -\frac{\mu_y}{2\pi} \left\{ \frac{\gamma_2(x_i(s) - x_j(p))}{r_{ij}^2(s, p)} + \int_0^{+\infty} \left([2kG_y(\beta^2 - \lambda^2) \sin h(\beta h_1) \alpha \cos h(\alpha y_j(p)) \right. \right. \\ &\quad \left. \left. + 2\mu_y \alpha^2 \sin h(\alpha y_j(p)) \{k\lambda \sin h(\beta h_1) - k\beta \cos h(\beta h_1) - G_y(\beta^2 - \lambda^2) \sin h(\beta h_1)\} \right] \right. \\ &\quad \left. \times \frac{\sin h[\alpha(y_i(s) + h_2)]}{E(s)s^2} - \gamma_2 e^{-\gamma_2 s(y_j(p) - y_i(s))} \right\} \sin(s(x_i(s) - x_j(p))) ds \quad -h_2 < y < \zeta \end{aligned} \quad (13)$$

By substituting Eq. (11) and (13) into Eq. (12), we obtain the following singular integral equations:

$$\begin{aligned} \sum_{j=1}^N \int_{-1}^1 -\frac{\mu_y}{\pi} \left\{ \frac{\gamma_2(x_i(s) - x_j(p))}{r_{ij}^2(s, p)} + \int_0^{+\infty} \left([kG_y(\beta^2 - \lambda^2) \sin h(\beta h_1) \alpha \cos h(\alpha y_i(s)) + \mu_y \alpha^2 \sin h(\alpha y_i(s)) \right. \right. \\ \left. \left. \times \{k\lambda \sin h(\beta h_1) - k\beta \cos h(\beta h_1) - G_y(\beta^2 - \lambda^2) \sin h(\beta h_1)\} \right] \right. \\ \left. \times \frac{\sin h[\alpha(y_j(p) + h_2)]}{E(s)s^2} - \gamma_2 e^{-\gamma_2 s(y_i(s) - y_j(p))} \right\} \sin(s(x_i(s) - x_j(p))) ds \Big\} B_{zj}(p) l_j dp = \tau_0 \quad \zeta < y < 0 \\ \sum_{j=1}^N \int_{-1}^1 -\frac{\mu_y}{2\pi} \left\{ \frac{\gamma_2(x_i(s) - x_j(p))}{r_{ij}^2(s, p)} + \int_0^{+\infty} \left([2kG_y(\beta^2 - \lambda^2) \sin h(\beta h_1) \alpha \cos h(\alpha y_j(p)) + 2\mu_y \alpha^2 \sin h(\alpha y_j(p)) \right. \right. \\ \left. \left. \times \{k\lambda \sin h(\beta h_1) - k\beta \cos h(\beta h_1) - G_y(\beta^2 - \lambda^2) \sin h(\beta h_1)\} \right] \frac{\sin h[\alpha(y_i(s) + h_2)]}{E(s)s^2} \right. \\ \left. \left. - \gamma_2 e^{-\gamma_2 s(y_j(p) - y_i(s))} \right\} \sin(s(x_i(s) - x_j(p))) ds \Big\} B_{zj}(p) l_j dp = \tau_0 \quad -h_2 < y < \zeta \end{aligned} \quad (14)$$

According to the definition of dislocation, the crack opening displacement across the j th crack is given by

$$w_j^-(s) - w_j^+(s) = \int_{-1}^s l_j B_{zj}(p) dp \quad j = 1, 2, 3, \dots, N \quad (15)$$

The single-valued property of the displacement field out of an embedded crack surface yields the following closure conditions for embedded cracks

$$l_j \int_{-1}^1 B_{zj}(p) dp = 0, \quad j = 1, 2, 3, \dots, N. \quad (16)$$

The system of integral Eqs. (14) and (16) is solved to determine the dislocation density functions $B_{zj}(p)$. This task is taken up by the methodology developed by Erdogan et al. [24]. The stress fields in the neighborhood of crack tips behave like $1/\sqrt{r}$ where r is the distance from the crack tip. Therefore, the dislocation densities are taken as

$$B_{zj}(p) = \frac{g_{zj}(p)}{\sqrt{1-p^2}}, \quad -1 \leq p \leq 1 \quad j = 1, 2, 3, \dots, N \quad (17)$$

Substituting Eq. (17) into Eqs. (14) and (16) and discretizing the domain, $-1 \leq p \leq 1$, by $m + 1$ segments, the integral equations are reduced to the following system of $N \times 2m$ linear algebraic equations

$$\begin{bmatrix} A_{11} & A_{12} & \cdots & A_{1N} \\ A_{21} & A_{22} & \cdots & A_{2N} \\ \vdots & \vdots & \ddots & \vdots \\ A_{N1} & A_{N2} & \cdots & A_{NN} \end{bmatrix} \begin{bmatrix} g_{z1}(p_n) \\ g_{z2}(p_n) \\ \vdots \\ g_{zN}(p_n) \end{bmatrix} = \begin{bmatrix} q_1(s_r) \\ q_2(s_r) \\ \vdots \\ q_N(s_r) \end{bmatrix} \quad (18)$$

where the collocation points are

$$s_r = \cos\left(\frac{\pi r}{m}\right) \quad r = 1, 2, \dots, m-1, \quad p_n = \cos\left(\frac{\pi(2n-1)}{2m}\right), \quad n = 1, 2, \dots, m \quad (19)$$

The components of matrix and vectors in (18) are

$$A_{ij} = \frac{1}{m} \begin{bmatrix} K_{ij}(s_1, p_1) & K_{ij}(s_1, p_2) & \cdots & K_{ij}(s_1, p_m) \\ K_{ij}(s_2, p_1) & K_{ij}(s_2, p_2) & \cdots & K_{ij}(s_2, p_m) \\ \vdots & \vdots & \ddots & \vdots \\ K_{ij}(s_{m-1}, p_1) & K_{ij}(s_{m-1}, p_2) & \cdots & K_{ij}(s_{m-1}, p_m) \\ \pi \delta_{ij} \Delta_i(p_1) & \pi \delta_{ij} \Delta_i(p_2) & \cdots & \pi \delta_{ij} \Delta_i(p_m) \end{bmatrix}$$

$$g_{zj}(p_n) = [g_{zj}(p_1) \quad g_{zj}(p_2) \quad \cdots \quad g_{zj}(p_m)]^T$$

$$q_j(s_r) = [\sigma_{nz}(x_j(s_1), y_j(s_1)) \sigma_{nz}(x_j(s_2), y_j(s_2)) \cdots \sigma_{nz}(x_j(s_{m-1}), y_j(s_{m-1})) \quad 0]^T \quad (20)$$

where δ_{ij} in the last row of A_{ij} is the Kronecker delta and superscript stands T for the transpose of a vector. The stress intensity factors at the tip of i th crack in terms of the crack opening displacement reduce to

$$k_{III Li} = \frac{\sqrt{2}}{4} \mu(y_{Li}) \lim_{r_{Li} \rightarrow 0} \frac{w_j^-(s) - w_j^+(s)}{\sqrt{r_{Li}}},$$

$$k_{III Ri} = \frac{\sqrt{2}}{4} \mu(y_{Ri}) \lim_{r_{Ri} \rightarrow 0} \frac{w_j^-(s) - w_j^+(s)}{\sqrt{r_{Ri}}}, \quad (21)$$

where subscripts L and R designate, the left and right tips of a crack, respectively. The geometry of a crack implies:

$$r_{Li} = [(x_i(s) - x_i(-1))^2 + (y_i(s) - y_i(-1))^2]^{\frac{1}{2}},$$

$$r_{Ri} = [(x_i(s) - x_i(1))^2 + (y_i(s) - y_i(1))^2]^{\frac{1}{2}}. \quad (22)$$

In order to take the limits for $r_{Li} \rightarrow 0$ and $r_{Ri} \rightarrow 0$, we should let, in Eq. (21), the parameter $s \rightarrow -1$ and $s \rightarrow 1$, respectively. The substitution of (17) into (15), and the resultant equations and Eq. (22) into Eq. (21) in conjunction with the Taylor series expansion of functions $x_i(s)$ and $y_i(s)$ around the points $s = \pm 1$ results in the modes III stress intensity factors for embedded cracks as

$$k_{III Li} = \frac{f \mu(y_{Li})}{2} ((x'_i(-1))^2 + (y'_i(-1))^2)^{\frac{1}{4}} g_{zi}(-1),$$

$$k_{III Ri} = -\frac{f \mu(y_{Ri})}{2} ((x'_i(1))^2 + (y'_i(1))^2)^{\frac{1}{4}} g_{zi}(1), \quad i = 1, \dots, N \quad (23)$$

Eq. (17) is substituted into Eq. (14) and (16) and the resultant equations are solved for the $g_{zj}(p)$ via the technique developed by Erdogan et al. [24]. The results for $g_{zi}(\mp 1)$ should be substituted into Eq. (23) to determine stress intensity factors.

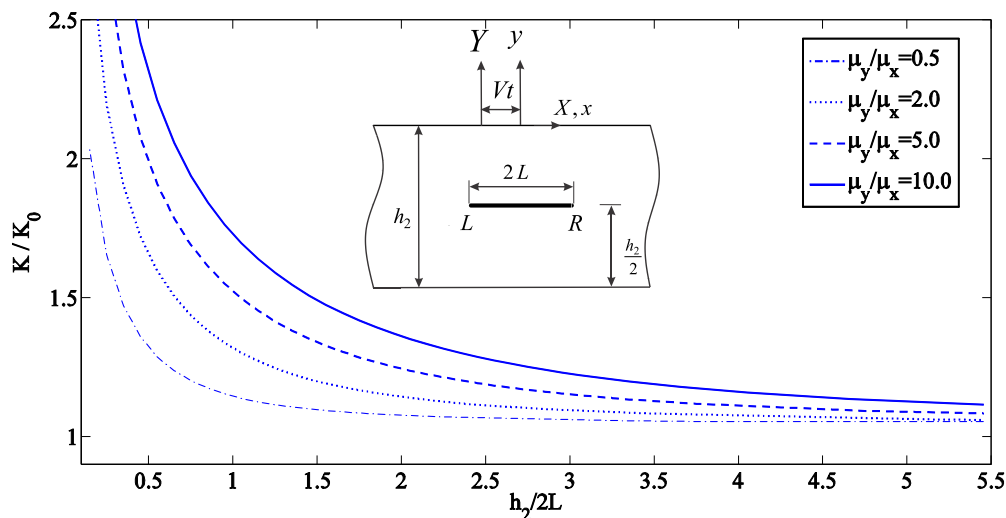


Fig. 2. Variation of dynamic stress intensity factor for multiple ratio of shear modulus.

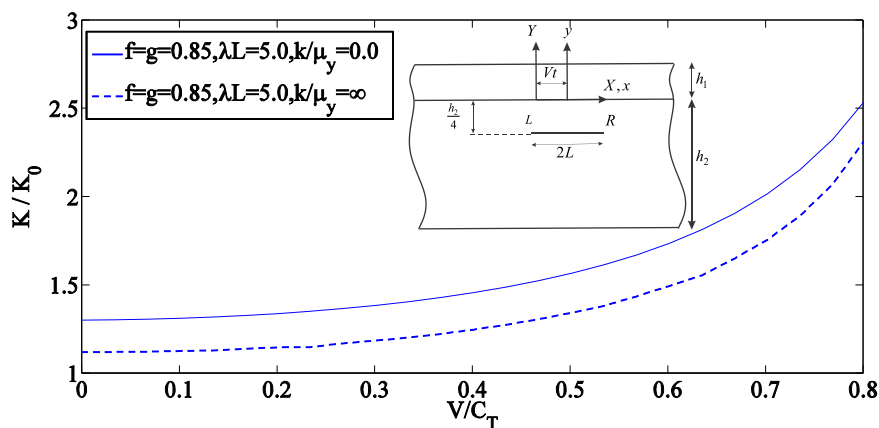


Fig. 3. Variation of dynamic stress intensity factor with bonding coefficient.

4. Results and discussions

The theoretical analysis described in the previous sections is used to investigate the effect of the pertinent parameters upon the dynamic stress intensity factors of the multiple moving cracks. In particular, it is interesting to explore the effect of the bonding condition. For that purpose, numerical calculations are carried out for three kinds of coating. The results of the present paper are shown in Figs. 2–8. The applied load in all examples is the constant anti-plane shear traction on the top and bottom face of the layers. From the results, it can be observed that the dynamic stress intensity factors not only depend on the crack length, properties of the material and speed of crack propagating, but also depend on the bonding coefficient.

The validity of formulation is examined by obtaining stress intensity factor for a stationary crack situated parallel to the boundaries of an isotropic strip. By setting $V = 0$ and $g = f = 1$, the ratio K/K_0 is obtained which is identical to that reported by Fotuhi and Fariborz [25] who have used the distributed dislocation technique as well. Furthermore, the present solution ($V = 0$) is in close agreement with the solution given in [23]. As a final check, the present formulation is simplified to the case of a moving crack located in the center-line of an orthotropic strip. It is observed that the curves for K/K_0 versus $h_2/2L$ coincide with those reported by Danyluk and Singh [4]. In the following examples, a cracked orthotropic substrate with imperfect non-homogeneous coating is analyzed.

First, we restrict our attention to the moving crack problem in an orthotropic layer with FGM orthotropic coating in the limiting condition $k = 0$ and $k = \infty$. Fig. 3 shows the effect of the crack propagation speed V/C_T upon dimensionless stress intensity factors. The crack is propagating parallel to the strip surfaces with constant velocity V at time $t = 0$, in the positive x -direction. According to this figure, the dynamic stress intensity factor is increased with the increase of the speed of crack propagation (V/C_T). Two types of FGM orthotropic coating were used, for $k/\mu_y = 0$ the problem reduces to an orthotropic

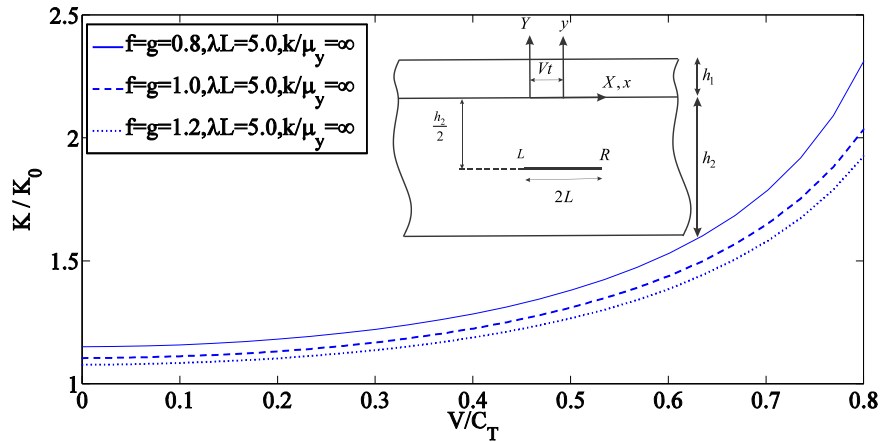


Fig. 4. Variation of DSIF with crack propagation speed for multiple ratio of shear modulus.

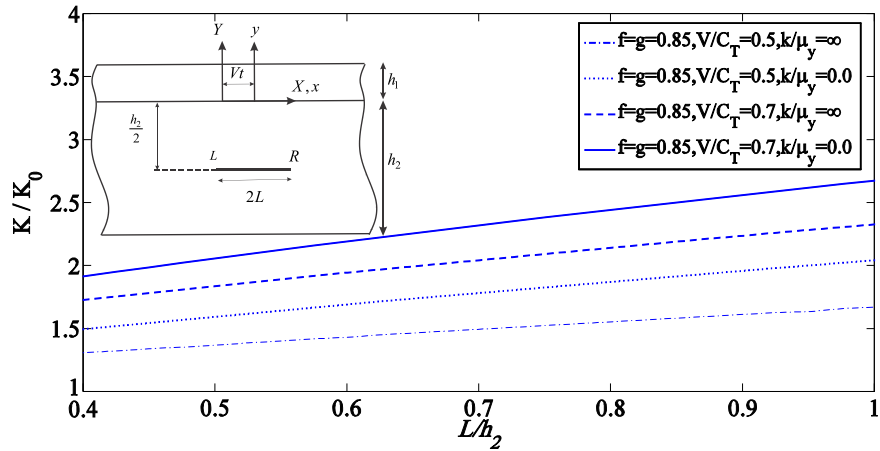


Fig. 5. Variation of DSIF with crack length.

strip weakened by crack without reinforcement and for $k/\mu_y = \infty$, the layers are perfectly bonded. It is observed that K/K_0 decreases with the increasing of the bonding coefficient k/μ_y .

The variations of the stress intensity factors versus the crack propagation speed V/C_T are given in Fig. 4. Several combinations of shear modulus ratio of coating g and substrate f , with the fixed values of $h_1/h_2 = L/h_2 = 0.1$ are considered for a perfectly bonded coating. As demonstrated in Fig. 4, in the orthotropic layer, the stiffer material in the crack direction attenuates dynamic stress intensity factor. Significant effect of material property upon K/K_0 can be observed with variation of crack propagation speeds.

The effect of crack length on the behavior of the moving crack is provided in Fig. 5 for two limiting values of bonding coefficient k/μ_y . It can be seen that, K/K_0 increases significantly with increasing of the crack length while it decreases with the increasing of k/μ_y . It can be concluded that for these layers, parameter k/μ_y has a great influence on the dynamic stress intensity factor.

The effect of material property of substrate, i.e. f , is investigated in more details in Fig. 6. The dynamic stress intensity factor is influenced considerably by the change of shear modulus ratio.

Next examples (Figs. 7 and 8) demonstrate the capability of the distributed dislocation technique in the analysis of the interactions of multiple cracks. Consider the case where the two collinear moving cracks are located on the center-line of the orthotropic strip. The graph given in Fig. 7 shows the variation of DSIFs, versus l/h_y where $2a$ is the distance between the two approaching crack tips. Note that as the length of the cracks increase, the amplitudes of the dimensionless stress intensity factors increase with a faster rate. For other values of the crack propagation speed, similar trend of variation of K/K_0 with different values are observed. In this case, the DSIFs of the inner crack tips are bigger than those of the outer crack tips because of the interaction of two collinear cracks.

In the last example, we restrict our attention to the two off-center crack configuration. The anti-plane behavior of a coating–substrate layer weakened by two off-center cracks, with equal lengths $L = 0.25h_2$, is studied. In this case, we take $a/h_2 = 0.125$ and study the effect of the crack propagation speed. The variation of dynamic stress intensity factors of crack L_2, R_2 is much smaller than that of crack L_1, R_1 . This attributes to weak interaction of cracks. Further, due to the interface interaction, the intensity factors of the first crack are higher than those for the second crack.

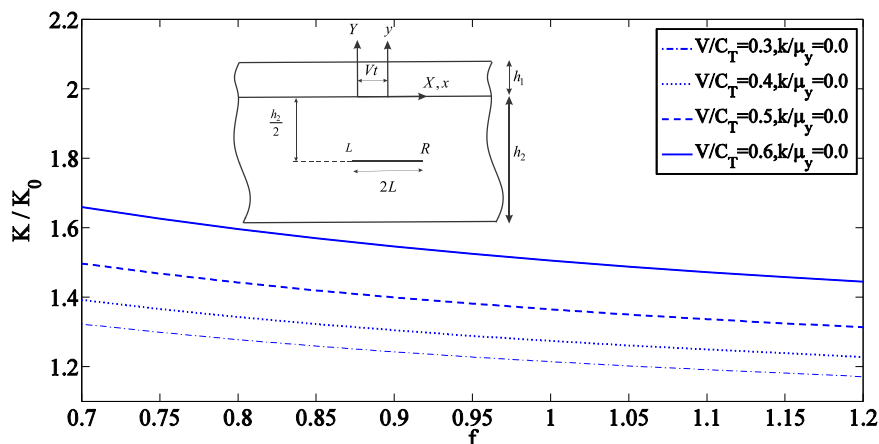
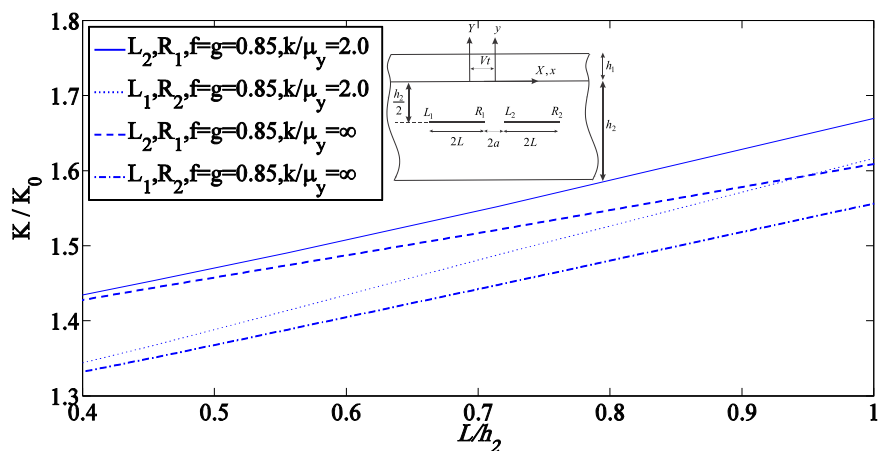
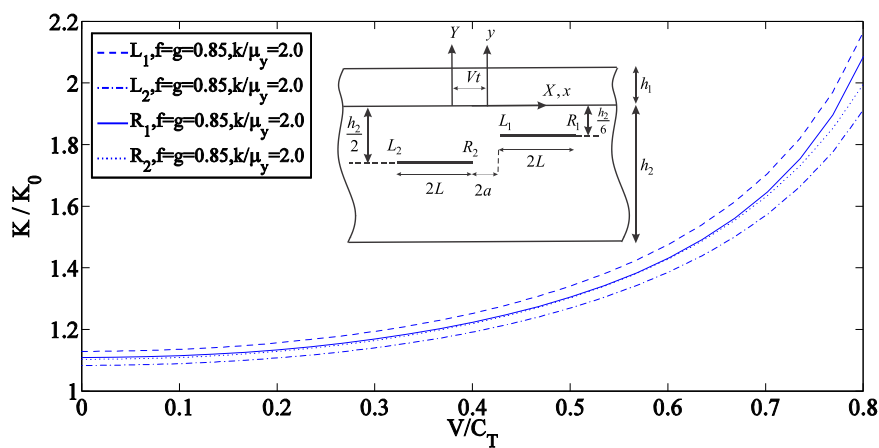
Fig. 6. Variation of DSIF with f .Fig. 7. Variation of DSIFs of two collinear moving cracks versus L/h_2 .

Fig. 8. Variation of DSIFs of two off-center moving cracks versus crack propagation speed.

5. Conclusions

This paper deals with stress analysis of a medium composed of an orthotropic substrate weakened by moving cracks and reinforced by a non-homogenous coating. A linear spring model is applied to simulate interfacial imperfection. In summary, the dynamic stress intensity factors of crack tips in orthotropic layer depend on various factors such as material, geometry and

interface properties. Considering different interfaces, it is demonstrated that the stress intensity factor decreases with the increase of the stiffness coefficient at the interface of two materials.

References

- [1] L.B. Freund, *Dynamic Fracture Mechanics*, Cambridge University Press, 1998.
- [2] G.C. Sih, *Elastodynamic Crack Problems (Mechanics of Fracture 4)*, Noordhoff, Leyden, 1977.
- [3] G.C. Sih, E.P. Chen, Moving cracks in layered composites, *Int. J. Eng. Sci.* 20 (1982) 1181–1192.
- [4] H.T. Danyluk, B.M. Singh, Closed form solutions for a finite length crack moving in an orthotropic layer of finite thickness, *Lett. Appl. Eng. Sci.* 22 (1984) 637–644.
- [5] X.D. Wang, S.A. Meguid, On the dynamic crack propagation in an interface with spatially varying elastic properties, *Int. J. Fract.* 69 (1994) 87–99.
- [6] Y. Wang, J.G. Williams, Dynamic crack growth in TDCB specimens, *Int. J. Mech. Sci.* 38 (1996) 1073–1088.
- [7] S.A. Meguid, X.D. Wang, L.Y. Jiang, On the dynamic propagation of a finite crack in functionally graded materials, *Eng. Fract. Mech.* 69 (2002) 1753–1768.
- [8] L.Y. Jiang, X.D. Wang, On the dynamic propagation in an interphase with spatially varying elastic properties under in-plane loading, *Int. J. Fract.* 114 (2002) 225–244.
- [9] S. Chi, Y.L. Chung, Cracking in coating-substrate composites with multi-layered and FGM coating, *Eng. Fract. Mech.* 70 (2003) 1227–1243.
- [10] X.S. Bi, J. Cheng, X.L. Chen, Moving crack for functionally graded material in an infinite length strip under anti-plane shear, *Theor. Appl. Fract. Mech.* 39 (2003) 89–97.
- [11] L. Ma, L.Z. Wu, L.C. Guo, On the moving Griffith crack in a non-homogeneous orthotropic strip, *Int. J. Fract.* 136 (2005) 187–205.
- [12] S. Das, Interaction of moving interface collinear Griffith cracks under antiplane shear, *Int. J. Solids Struct.* 43 (2006) 7880–7890.
- [13] B.M. Singh, J. Rokne, J. Vrbik, R.S. Dhaliwal, Finite Griffith crack propagating in a non-homogeneous medium, *Eur. J. Mech. A Solids* 25 (2006) 867–875.
- [14] B.L. Wang, J.C. Han, A moving crack in a non-homogeneous material, *Acta Mech. Solida Sin.* 19 (2006) 223–230.
- [15] B.L. Wang, J.C. Han, A mode III moving crack between a functionally graded coating and homogeneous substrate, *J. Mech. Mater. Struct.* 1 (2006) 649–661.
- [16] Z. Cheng, Z. Zhong, Analysis of a moving crack in a functionally graded strip between two homogeneous layers, *Int. J. Mech. Sci.* 49 (2007) 1038–1046.
- [17] F. Greco, P. Lonetti, Mixed mode dynamic delamination in fiber reinforced composites, *Compos. Part B Eng.* 40 (2009) 379–392.
- [18] D. Bruno, F. Greco, P. Lonetti, Dynamic mode I and II crack propagation in fiber reinforced composites, *Mech. Adv. Mater. Struct.* 16 (2009) 442–455.
- [19] Z. Cheng, D. Gao, Z. Zhong, Crack propagation in functionally graded coating with arbitrarily distributed material properties bonded to homogeneous substrate, *Acta Mech. Solida Sin.* 23 (2010) 437–446.
- [20] R. Bagheri, M. Ayatollahi, E. Asadi, Dynamic fracture analysis of multiple defects in an imperfect FGM coating-substrate layers, *Int. J. Mech. Sci.* 75 (2013) 55–65.
- [21] D.A. Hills, P.A. Kelly, D.N. Dai, A.M. Korsunsky, *Solution of Crack Problems: The Distributed Dislocation Technique*, Kluwer Academic Publishers, 1996.
- [22] E. Asadi, S.J. Fariborz, A.R. Fotuhi, Anti-plane analysis of orthotropic strips with defects and imperfect FGM coating, *Eur. J. Mech. A Solids* 34 (2012) 12–20.
- [23] J. Weertman, *Dislocation Based Fracture Mechanics*, World Scientific Publishing Co., Singapore, 1996.
- [24] F. Erdogan, G.D. Gupta, T.S. Cook, Numerical Solution of Singular Integral Equations, *Method of Analysis and Solution of Crack Problems*, in: G.C. Sih (Ed.), Noordhoff, Leyden, Holland, 1973.
- [25] A.R. Fotuhi, S.J. Fariborz, Anti-plane analysis of a functionally graded strip with multiple cracks, *Int. J. Solids Struct.* 43 (2006) 1239–1259.